

# Chemical space exploration with molecular genes and machine learning

Bing Huang and O. Anatole von Lilienfeld\*

*Institute of Physical Chemistry and National Center for Computational Design and Discovery of Novel Materials (MARVEL),  
Department of Chemistry, University of Basel, Klingelbergstrasse 80, 4056 Basel, Switzerland*

(Dated: December 14, 2024)

Given sufficient examples, recently introduced machine learning (ML) models enable rapid, yet arbitrarily accurate, molecular property calculations of new molecules. Extrapolation to molecules of arbitrary size and composition, however, is prohibitive due to the specific chemistries imposed during training. We rectify this problem by removing redundancies as detected through chemical similarity among molecular fragments. Training set selection of the most relevant fragments—the “genes” of chemistry—results in real-time ML predictions for query molecules of arbitrary size, structure, and composition. We demonstrate this for covalently and non-covalently bonded systems, and reach prediction errors on par with experimental uncertainty, after training on very few genes. Systems studied include two dozen large biomolecules, one thousand medium sized organic molecules, common polymers, large water clusters, doped *h*BN sheets, bulk silicon, and Watson-Crick DNA base pairs. The “genes” extend Mendeleev’s table to also account for chemical environments of atoms, and represent an important stepping stone to virtual chemical space exploration campaigns with unprecedented speed and accuracy.

## INTRODUCTION

The basic concept of fundamental building blocks, determining the behaviour of matter through their specific combinations, has had a profound impact on our understanding of particle physics (quarks) [1], electronic structure of atoms and molecules (elemental particles) [2], or proteins and genetic codes (amino and nuclear acids) [3]. Within the molecular sciences, the transferability among functional groups has enabled synthetic chemists to reach remarkably precise control over intricate complex atomistic processes. Theoretical chemistry has yet to transform such chemical intuition into an equally efficient and transferable approach. If universally predictive this would manifest a profound understanding of chemistry, and enable the computational exploration of chemical space [4] with unprecedented scale and precision. Important molecular and materials design challenges could then be tackled, possibly alleviating many of today’s pressing problems due to lack of new drugs, clean water, or efficient catalysts.

Unfortunately, reliable and generic virtual exploration campaigns in chemical space remain prohibitive due to the considerable computational cost of state-of-the-art quantum methods, such as density functional theory (DFT) [5, 6]. Within the last decade, novel machine learning (ML) models have introduced alternative ways to efficiently tackle long-standing fundamental problems in physics and chemistry [7–18]. None of these ML models, however, offers the scalability required to screen chemical compounds of arbitrary size and composition, while various *ab initio* strategies have already been proposed to address this issue [19–25]. Unfortunately, the latter methods typically either trade predictive transferability, or continue to suffer from steep scaling prefactors. We resolve this outstanding challenge through a

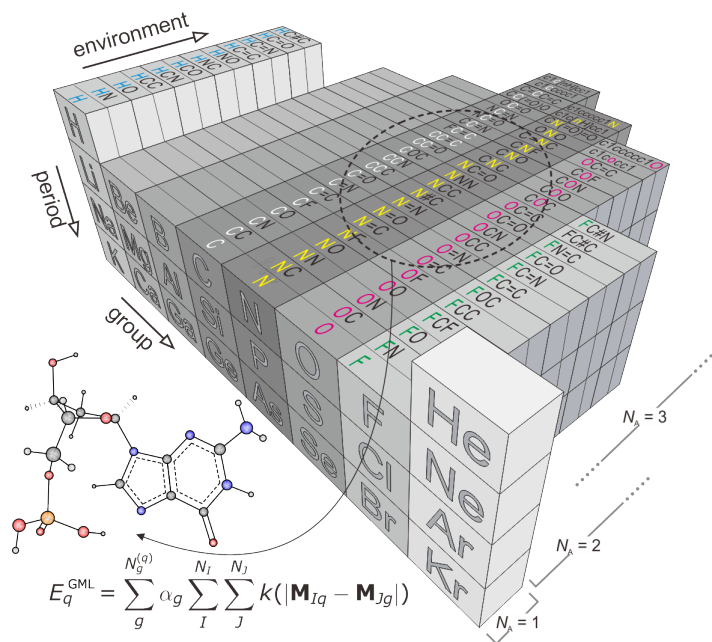


Figure 1. Illustration of the “genes” of chemistry as a compositional extension of the periodic table (for clarity only shown for main-group elements C, H, O, N, and F) in terms of SMILES strings arranged in increasing number of surrounding elements, and covering typical chemical environments. Within our gene machine learning approach, the energy of a query compound  $E_q$  (exemplary guanine nucleotide on display) is expanded in  $N_g$  genes, the double summation being weighted by kernel ridge regression coefficients  $\{\alpha_g\}$ , and quantifying the similarity  $k$  between all respective  $N_I$  and  $N_J$  atoms in query and gene molecule  $\mathbf{M}_q$  and  $\mathbf{M}_g$ .

combination of the notion of molecular fragments, machine learning and quantum chemistry reference results. Since fragments repeat throughout chemical space, independent of the specific query molecule at hand, they

can be viewed as “genes” of chemistry. By accounting for all possible chemical environments of each element these genes effectively extend the dimensionality of the periodic table (See Fig. 1). To demonstrate the applicability and transferability of our model, we present results for a multitude of systems, including two dozens large biomolecules, one thousand medium sized organic molecules, five common polymers, six water clusters with up to 280 molecules, three doped *h*-BN sheets, bulk silicon, and Watson-Crick bonded DNA base pairs. We are not aware of any alternative approach which provides similar convergence behaviour and extrapolative capabilities.

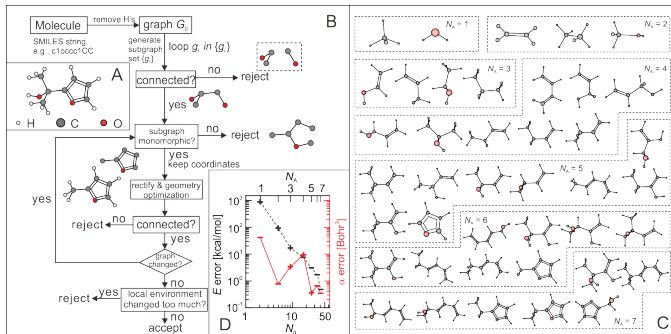


Figure 2. Illustration of the gene selecting algorithm, exemplified for the prediction of molecule 2-(furan-2-yl)propan-2-ol (A); (B) Flow-chart for graph-based selection of genes; (C) Selected genes for query molecule; (D) Absolute error of predicted total energy (black) and isotropic static polarizability (red) as a function of number of genes in training set ( $N_g$ ) or number of heavy atoms per gene ( $N_A$ , not counting hydrogens), respectively. Plus and minus symbols indicate positive and negative errors, respectively.

**Method** When breaking up large query molecules, e.g. through cascades of isodesmic reactions, increasingly smaller and more common molecular fragments are obtained whose summed up energy will increasingly deviate from query. Our *Ansatz* corresponds to the reverse: Starting very small, increasingly larger molecular “genes” are being included in training, resulting in increasingly accurate ML models. By selecting small genes which retain the same local chemical environment as in the query molecule the training set size is minimized.

In Fig. 2 we illustrate the “gene” ML (GML) approach for predicting the total potential energy of the organic molecule named 2-(furan-2-yl)propanol ( $C_7H_{10}O_2$ ): The GML prediction improves systematically as more and larger genes are being selected through the sub-graph matching algorithms, reaching  $\sim 1.5$  kcal/mol prediction error with no more than 34 genes with at most 6 heavy atoms each. To exceed chemical accuracy ( $\sim 1$  kcal/mol prediction error) the training set has to include 7 additional genes with 7 heavy atoms each. By comparison, tens of thousands of training molecules are needed to reach similar prediction errors using conven-

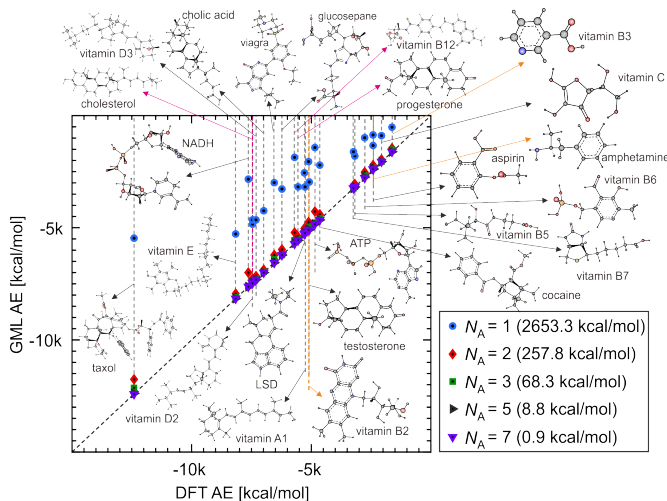


Figure 3. Applicability of GML, demonstrated by systematic improvement of predicted atomization energies (AE) for two dozen important biomolecules using increasingly larger genes. The inset specifies the maximal number of heavy atoms ( $N_A$ , not counting hydrogens) per gene, as well as resulting MAE. Chemical, DFT, and force-field accuracy is roughly reached for genes with 7, 5 and 3 heavy atoms, respectively. All genes used are specified in supplementary materials.

tionally trained ML models trained on randomly selected molecules [10, 18]. Inspection of the selected genes reveals that all “local chemistries”, present in the molecule, have been dialled in. For example, alcohols with respectively  $sp^3$ - and  $sp^2$ -hybridized carbon atoms in vicinal and geminal position to the hydroxy group are present among all genes with more than three heavy atoms. While the prediction error in Fig. 2D decreases systematically with gene and training set size, the sign indicates that the query energy is underestimated by GML for smaller genes (up to 3 heavy atoms), and overestimated for larger genes (starting with 4 heavy atoms which can form conjugated double bonds). Furthermore, due to kernels being property invariant, GML models of other properties can trivially be generated using the same selection of genes. To convey this fact, we also show the prediction error for the isotropic static molecular polarizability in Fig. 2D: The learning curve resembles a damped oscillator, converging towards the target number.

Note that in comparison to more conventional isodesmic construction approaches [25] our GML model differs by (a) the selection algorithm which automatically solves the isodesmic partitioning problem, (b) the specific linear combination of energy contributions, appropriately weighted through use of kernel ridge regression, and (c) averaging out combinatorially many fragmentation schemes which represent the buffer regions linking different genes (see supplementary material for more detail).

To make use of an efficient GML implementation, we

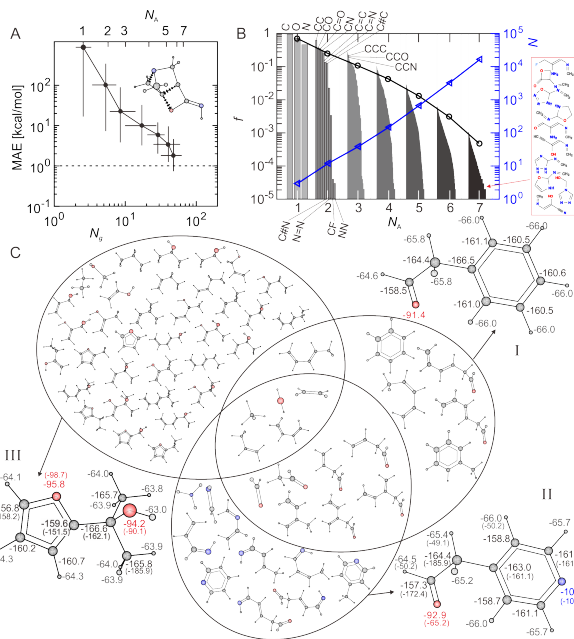


Figure 4. The genes of organic chemistry: (A) Mean absolute prediction error (circles) of total potential energy of 1k organic molecules (with  $N_A = 9$  from QM9 [26]) as a function of number of heavy atoms per gene ( $N_A$ , not counting hydrogens) or genes ( $N_g$ ) in training set. Standard deviations with respect to error and  $N_g$  are also shown. The inset shows a typical outliers with high strain. (B) Left axis: Frequency of genes ( $f = \text{number of occurrence}/\text{number of query molecules}$ ) in descending order; right axis: Number of query molecules  $N$ , both as a function of  $N_A$  of genes. Insets specify the most and least frequent genes. (C) Genes for 2-phenylacetaldehyde (I), 2-(furan-2-yl)propan-2-ol (II) and 2-(pyridin-4-yl)acetaldehyde (III). Overlapping regions correspond to shared genes. Numbers indicate atomic energies regressed by GML, or Morse-potential (in brackets) where meaningful and for comparison.

developed a specific interatomic many-body representation of atoms in molecules. Due to its popularity we have used hybrid DFT for training and validation throughout. We note that the choice of reference is irrelevant for GML, any other level of theory could have been used just as well. To demonstrate this fact, we have included some Hartree-Fock, MP2, and CCSD(T) GML learning curves in the supplementary materials. More specifics and computational details are given below and in Supplementary Materials.

**Results and Discussion** To illustrate the efficiency and applicability of GML for making predictions of molecules of arbitrary size and composition, we first discuss the prediction of total energies for two dozen large and important biomolecules, such as cholesterol, cocaine, taxol, or NADH. True versus predicted energies are shown in Fig. 3 for various GML models trained on sets of genes containing  $N_A = 1, 2, 3, 5,$  and  $7$  heavy atoms. Systematic improvement of predictive accuracy is found reaching mean

absolute errors typically associated with force-fields, density functional theory, or experimental thermochemistry for genes with 3, 5, or 7 heavy atoms, respectively. For smaller query molecules with rigid and strain-less structure and similar chemical environments of the constituting atoms, e.g., vitamin B3 with only 9 heavy atoms, the prediction error decreases faster with gene size than for more complex molecules, and chemical accuracy is reached with less than one hundred genes in total (see supplementary material for the specific training set sizes). Not surprisingly, large and complex molecules with diverse atomic chemical environments, such as NADH, require substantially more genes to reach the same level of accuracy. We note that the GML prediction error always converges from above on the scale of atomization energies.

When exploring chemical space, however, one invariably faces the problem of severe selection bias due to the unfathomably large scale resulting from all the possible combinations of atom types and coordinates. In order to rule out the possibility of above results being coincidental, we have investigated the GML performance for one thousand diverse organic query molecules made up of 9 heavy atoms. All query molecules were drawn at random from the recently published QM9 dataset [26, 27], which consists of coordinates and electronic properties of 134k organic molecules calculated at the hybrid DFT level of theory. While QM9 certainly constitutes only a small and primitive subset of chemical space [4, 28], our conclusions are drawn without loss of generality: Any other molecular data set could have been chosen just as well.

After gene training selection and subsequent training, we find again that prediction errors of atomization energies systematically decrease with number and size of genes (See Fig. 4A). Encouragingly, standard deviations tend to decrease together with the mean absolute error, and the MAE reaches 1.8 kcal/mol for genes with up to 7 heavy atoms. We reiterate that such training set sizes are two to three orders of magnitude smaller than for conventional neural network or kernel ridge regression models which rely on random sampling and which do not scale [16, 18]. Examining molecules one by one, we find that largest deviations correspond to molecules containing highly strained fragments, such as in inset of Fig. 4A. In order to properly account for strained query molecules, the training set requires inclusion of relatively large genes with similarly strained local motifs.

Application of the gene selection algorithm to the 110k organic molecules in QM9 with 9 heavy atoms results in a grand total of  $\sim 21k$  genes (all specified in the Supplementary Material). The normalized frequency distribution of these genes is shown in Fig. 4B, together with the exponentially growing number of molecules in QM9. As one would expect, the smaller the gene the more frequently it will be selected, and for a given gene size high carbon content is more frequent than high oxygen or ni-

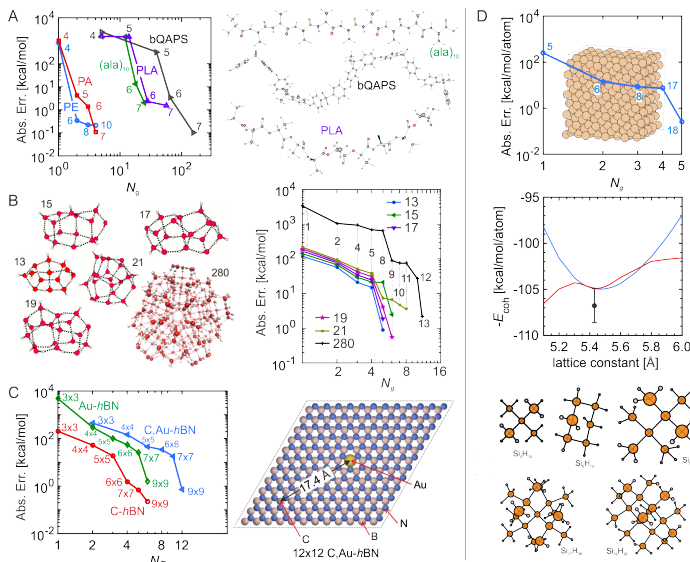


Figure 5. Scalability of the GML model, illustrated by learning curves for (A) 6 polymers, including polyethylene (PE, with 28 monomers), polyacetylene (PA, with 15 monomers), alanine peptide ((ala)<sub>10</sub>), polylactic acid (PLA, with 10 monomers) and the backbone of quaternary ammonium polysulphone (bQAPS, with 3 monomers); (B) 6 water clusters with number of water molecules being 13, 15, 17, 19, 21 and 280; (C) 2-D hexagonal BN sheets with one B atom replaced by gold (Au-*h*BN), or carbon (C-*h*BN), or two B atoms replaced by gold and carbon (Au,C-*h*BN). Absolute errors are shown for per unit cell; (D) bulk silicon, for which also shown in the figure are predicted and DFT cohesive energies versus lattice constants (middle panel, where the black solid dot and vertical line represent experimental values [29, 30] and uncertainty of  $E_{coh}$ , respectively), as well as the genes (bottom panel, i.e., Si clusters saturated by hydrogens). All genes not shown here are specified in supplementary material.

trogen content. A list and a movie, displaying the one thousand most frequent genes are provided in the supplementary materials. Conversely, the larger the gene the less likely that it will be selected for predicting a random query molecule. It is hence consistent that the ten least frequent genes, not shared by any pair of query molecules, represent rather pronounced chemical specificity (right inset Fig. 4B). These results amount to numerical evidence that the fundamental idea of using “genetic” building blocks is meaningful for chemistry: The larger the query molecules and the smaller the genes, the more query molecules will share the same genes. These statistical results show how the GML model tames the curse of dimensionality in chemical space which grows exponentially with number of atoms [27, 28].

To deepen our understanding of chemistry, one can consider the number and nature of genes shared. They can serve as an intuitive measure of chemical similarity, as exemplified for three organic query molecules in Fig. 4C. The smallest genes are shared by all molecules,

and the more similar a pair of query molecules the larger the “genetic” overlap: Molecules I and II are more similar than I and III, which are more similar than II and III. Shared genes imply that GML predictions of other compounds will require fewer additional reference data. Another valuable insight obtained from GML is the transferability of regressed atomic energies: Local atoms possessing similar environments will contribute to similar degrees to the total energy, which also underpins the atoms-in-molecules theory [31]. To illustrate this atomic contributions to the GML estimated atomization energies are also printed for the three example molecules in Fig. 4C (see Supplementary Material for more detail). Encouragingly, their relative values are consistent with chemical intuition about covalent bonding. For example, there are three types of local oxygen environments (carbonyl, alcohol, and furane) contributing increasingly more to covalent binding ( $\sim 93$ , 94, and 96 kcal/mol, respectively), producing the same trend as one would expect for an atom sharing one double bond to carbon, two single bonds (carbon, hydrogen), and being in a conjugated environment (furane).  $sp^3$ -hybridized, aromatic, and  $sp^2$ -hybridized (in carbonyl) carbon atoms contribute with  $\sim 165$ , 160, and 158 kcal/mol, respectively. Hydrogen atoms range in their contribution from 64 to 66 kcal/mol. For comparison, we have also calculated corresponding energies using Morse potentials and parameters [32]. Overall fair agreement is found, suggesting the capability of GML to provide quantitative insight, previously exclusively accessible through physically motivated approximations. Note that, obviously, Morse potential based estimates of atomization energies of such molecules are dramatically worse than GML due to their averaged parameters, rigid functional form, and neglect of interatomic many-body effects.

After showcasing the performance of GML for organic molecules we now turn to the question of scalability. While some of the biomolecules in Fig. 3 are already substantially larger than the genes employed with no more than 7 heavy atoms, we have investigated the applicability of GML to very large systems in a more systematic fashion. Four different classes of systems, somewhat representative for the chemical space spanned by early main group elements, have been examined; and we have found that regardless of size and chemical nature, all prediction errors decrease systematically towards chemical accuracy as number and size of selected genes grows: (i) We have trained GML models to predict total potential energies of five common polymers with increasing size and chemical complexity (polyethylene ( $N_A = 26$ ), polyacetylene ( $N_A = 30$ ), alanine peptide ( $N_A = 50$ ), polylactic acid ( $N_A = 50$ ) and the backbone of quaternary ammonium polysulphone ( $N_A = 96$ )). The latter being essential for alkaline polymer electrolyte fuel cell (APEFC) technology [33]. Resulting learning curves in Fig. 5A exhibit a simple trend: The more chemically

complex the system, the more genes are selected and required in order to achieve predictive power. The chemically most complex polymer polysulphone requires nearly ten times more genes ( $\sim 200$ ) to reach chemical accuracy ( $\sim 1$  kcal/mol), than polyethylene, the chemically simplest polymer in our set ( $\sim 20$ ). (ii) Potential energies of water clusters consisting of 13, 15, 17, 19, 21 [34] and 280 [35] molecules have been predicted (see Fig. 5B). The prediction errors decay rapidly and systematically for all clusters and reach chemical accuracy with at most 10 genes. These results demonstrate the applicability of GML to also account for non-covalent hydrogen-bonding. (iii) We have examined periodic 2D materials, namely hexagonal BN sheets doped with carbon and gold (C-*h*BN; Au-*h*BN; C,Au-*h*BN), previously reported to have very high efficiency towards CO oxidation reaction [36] (see Fig. 5C). Due to substantial redundancy caused by underlying symmetries, GML prediction errors of total energies converge to chemical accuracy within at most 12 genes for the most complex C,Au-*h*BN doped variant. (iv) Symmetry plays an even more important role in crystalline bulk: To accurately predict the cohesive energy only 5 genes with no more than 18 silicon atoms are required (see Fig. 5D). Interestingly, a GML lattice scan produces even a reasonable minimum—despite the lack of distorted genes for training. We believe that this is due to the aforementioned fact that the GML model approaches the energy from above.

Logarithmized prediction errors of kernel ridge regression models decay linearly with logarithmized training set size [37], as long as training data and molecular representations are noise-free and unique, respectively [32]. All GML learning curves presented confirm the significant and general trend: GML off-set and slope improve dramatically over corresponding values for conventional ML models which do not scale and rely on random sampling of training molecules [10, 18]. The GML’s advantageous performance is likely to result from (i) a scalable building block approach, physically motivated by atoms-in-molecules theory [31], effectively reducing the formal dimensionality of the potential energy hyper surface in chemical space [28]. Dimensionality reductions are known to lead to steeper learning curves [38]; (ii) elimination of irrelevant or redundant training species through subgraph matching, which amounts to an optimization of training set composition, already shown to lead to substantial reduction in learning-curve off-set after using genetic algorithms [39]; (iii) a compact and minimalistic representation, based on interatomic many-body terms, which meets many crucial criteria identified in Ref. [32], and which also lowers the learning curve off-sets (see Supplementary Materials for more details).

Finally and out of curiosity, we have investigated the “genes” of DNA. More specifically, we have considered the Watson-Crick Cytosine-Guanine (GC) base pair (see Fig. 6E). While genes with no more than 7 heavy atoms

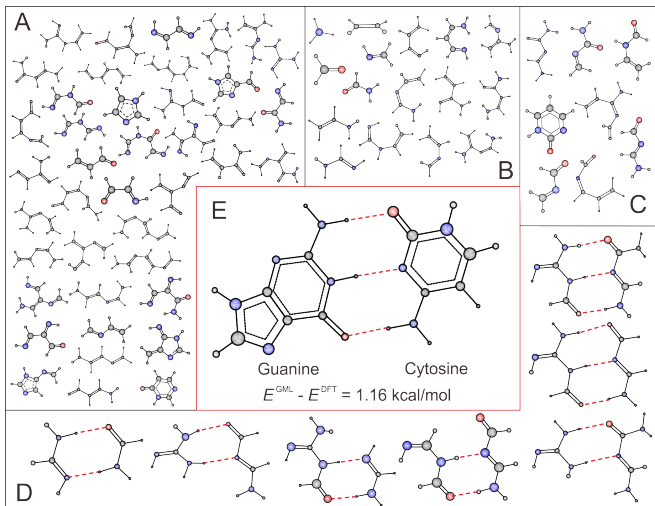


Figure 6. The genes of DNA, illustrated for Watson-Crick base-pair GC (E). (A) Genes of DNA base Guanine; (B) Genes shared by Cytosine and Guanine; (C) Genes of Cytosine; (D) Genes of Watson-Crick bonding pattern, all containing H-bonds. Trained on these genes, GML underestimates the DFT energy by 1.16 kcal/mol.

suffice to converge the energies for the individual base pairs, genes corresponding to truncated motifs of hydrogen bonds with up to twelve heavy atoms are necessary to reach chemical accuracy. Similar performance has been observed for the Watson-Crick bonded Adenine-Thymine base pair (See supplementary materials). It is not surprising that non-covalent bonding patterns, such as Watson-Crick bonding, require larger genes, as they extend over larger spatial domains. Furthermore, they also exhibit strong non-local effects through their conjugated moieties, implying the need for genes with multiple hydrogen bonds. Interestingly, to reach chemical accuracy it is not necessary to include genes which simultaneously contain aromatic fragments and hydrogen bonds, justifying previously made system choices for the study of nuclear quantum effects in DNA [40].

*Conclusion* We have introduced a molecular “gene” based machine learning (GML) model. GML is a Bayesian approach which infers the energy of *any* query compound, no matter its size or composition, based on a linear combination of properly weighted quantum chemistry results for its constituting building blocks. The electronic locality assumption (“nearsightedness”) [41] underpinning the GML approach, is exploited to systematically converge the effective energy contributions coming from the various fragments in a molecule. GML enables systematic convergence towards instantaneous energy predictions with unprecedented predictive power, on par with experimental uncertainties: We have demonstrated the versatility and robustness of GML for numerical error convergence results for predicted energies of two dozens large biomolecules with up to 96 heavy

atoms, one thousand organic molecules with nine heavy atoms, non-covalently bound systems consisting of water clusters and Watson-Crick DNA base pairs, as well as doped hexagonal BN sheets and bulk silicon.

Using genes with at most seven heavy atoms, chemical accuracy ( $\sim 1$  kcal/mol) is reached for most covalently bound systems. Since identical genes are common to diverse chemistries of arbitrary query molecules, our results suggest that a gene training set of very finite size and consisting of small to medium sized molecules will suffice to generate accurate and efficient GML models applicable to a practically infinite number of chemical systems. Therefore, we think it evident that high-level reference energies, such as post-Hartree-Fock or Quantum Monte Carlo methods, are no longer prohibitive for future GML models, effectively promising to finally sidestep the various issues which plague many of the common DFT approximations [42]. Future work will deal with developments of more sophisticated gene selection procedures to also account for distorted or reactive structures, predictions of other properties than total energies, and extensions of the gene pool to include further chemical elements, as well as open-shell, charged and electronically excited species.

*Technical details* For each atom  $I$  in query molecule  $q$  the model sums over genes with chemically similar atomic environments. More specifically, we rely on a kernel ridge regression model which approximates the energy difference between the truth and a baseline energy consisting of the sum of dressed atom energies ( $E_I^0$ ) which vary only among different elements and are obtained through fitting to the genes. For finite training set  $N_g$ ,

$$E_q^{\text{true}} \approx \sum_I E_I^0 + E_q^{\text{GML}}$$

where  $E_q^{\text{GML}}$  is the ML model specified in Fig. 1,  $\mathbf{M}_{Iq}$  and  $\mathbf{M}_{Jg}$  are the respective representations of atoms  $I$  and  $J$  in molecules  $q$  and  $g$ . The selection of  $N_g$  fragments is done independently for each query, and from scratch, following the algorithm shown in Fig. 2B and in the Supplementary Materials. Regression weights  $\{\alpha_g\}$  are generated “on-the-fly” through inversion of the covariance matrix  $K_{hg} = \sum_{KJ} k(|\mathbf{M}_{Kh} - \mathbf{M}_{Jg}|)$  between all training genes  $g$  and  $h$ . We use the Euclidean norm in Gaussian kernels with heuristically determined gene-dependent widths. The atomic environment of atom  $I$  is represented by the atomic SLATM (spectrum of London (two-body) and Axilrod-Teller-Muto (three-body) potentials). We refer to the supplementary materials for more details.

Selection of conformational genes for any query molecule is carried out according to the flowchart in Figure 2. A molecule is a graph ( $G$ ) defined by a set of vertices and edges  $\{V, E\}$  with different weights for  $V$  and  $E$  (which represent different atom/bond types). From this set we select a subset  $\{V_1, E_1\}$  (note that the 3D coordi-

nates of each vertex is kept the same as the corresponding part in parent molecule, i.e., the query molecule) and proceed only if the new set is monomorphic. The monomorphic fragments are relaxed after saturation with hydrogens. The gene is expelled if the geometry relaxation leads to major atomic rearrangements which result in a new molecular graph no longer monomorphic to the parent graph. This procedure is repeated until all subgraphs in  $G$  have been exhausted.

## SUPPLEMENTARY MATERIAL

More technical details as well as coordinates and energies are provided in the supplementary materials.

## ACKNOWLEDGEMENTS

O.A.v.L. acknowledges funding from the Swiss National Science foundation (No. PP00P2\_138932 and 407540.167186 NFP 75 Big Data). This research was partly supported by the NCCR MARVEL, funded by the Swiss National Science Foundation. Calculations were performed at sciCORE (<http://scicore.unibas.ch/>) scientific computing core facility at University of Basel.

---

\* anatole.vonlilienfeld@unibas.ch

- [1] R. P. Feynman, R. B. Leighton, and M. Sands, *The Feynman lectures on physics. Vol. 1* (Addison-Wesley, 1963).
- [2] R. M. Martin, *Electronic structure: basic theory and practical methods* (Cambridge university press, 2004).
- [3] J. B. Reece, L. A. Urry, M. L. Cain, S. A. Wasserman, P. V. Minorsky, R. B. Jackson, *et al.*, *Campbell biology* (Pearson Boston, 2011).
- [4] P. Kirkpatrick and C. Ellis, *Nature* **432**, 823 (2004).
- [5] P. Hohenberg and W. Kohn, *Phys. Rev.* **136**, B864 (1964).
- [6] K. Burke, *J. Chem. Phys.* **136**, 150901 (2012).
- [7] J. Behler and M. Parrinello, *Phys. Rev. Lett.* **98**, 146401 (2007).
- [8] M. Schmidt and H. Lipson, *Science* **324**, 81 (2009).
- [9] A. P. Bartók, M. C. Payne, R. Kondor, and G. Csányi, *Phys. Rev. Lett.* **104**, 136403 (2010).
- [10] M. Rupp, A. Tkatchenko, K.-R. Müller, and O. A. von Lilienfeld, *Phys. Rev. Lett.* **108**, 058301 (2012).
- [11] A. Rodriguez and A. Laio, *Science* **344**, 1492 (2014).
- [12] E. O. Pyzer-Knapp, K. Li, and A. Aspuru-Guzik, *Adv. Fun. Mat.* **25**, 6495 (2015).
- [13] F. A. Faber, A. Lindmaa, O. A. von Lilienfeld, and R. Armiento, *Phys. Rev. Lett.* **117**, 135502 (2016).
- [14] P. Raccuglia, K. C. Elbert, P. D. F. Adler, C. Falk, M. B. Wenny, A. Mollo, M. Zeller, S. A. Friedler, J. Schrier, and A. J. Norquist, *Nature* **533**, 73 (2016).
- [15] G. Carleo and M. Troyer, *Science* **355**, 602 (2017).

- [16] K. T. Schütt, F. Arbabzadah, S. Chmiela, K. R. Müller, and A. Tkatchenko, *Nat. Commun.* **8**, 13890 (2017).
- [17] S. Chmiela, A. Tkatchenko, H. E. Sauceda, I. Poltavsky, K. T. Schütt, and K.-R. Müller, *Sci. Adv.* **3**, e1603015 (2017).
- [18] F. A. Faber, L. Hutchison, B. Huang, J. Gilmer, S. S. Schoenholz, G. E. Dahl, O. Vinyals, S. Kearnes, P. F. Riley, and O. A. von Lilienfeld, arXiv preprint arXiv:1702.05532 (2017).
- [19] K. Kitaura, E. Ikeo, T. Asada, T. Nakano, and M. Uebayasi, *Chem. Phys. Lett.* **313**, 701 (1999).
- [20] S. Saebo and P. Pulay, *Annu. Rev. Phys. Chem.* **44**, 213 (1993).
- [21] M. Schütz, G. Hetzer, and H.-J. Werner, *J. Chem. Phys.* **111**, 5691 (1999).
- [22] W. Yang, *Phys. Rev. Lett.* **66**, 1438 (1991).
- [23] M. Gillan, D. Bowler, A. Torralba, and T. Miyazaki, *Comput. Phys. Comm.* **177**, 14 (2007).
- [24] R. M. Richard, K. U. Lao, and J. M. Herbert, *Acc. Chem. Res.* **47**, 2828 (2014).
- [25] K. Raghavachari and A. Saha, *Chem. Rev.* **115**, 5643 (2015).
- [26] R. Ramakrishnan, P. Dral, M. Rupp, and O. A. von Lilienfeld, *Sci. Data* **1**, 140022 (2014).
- [27] L. Ruddigkeit, R. van Deursen, L. C. Blum, and J.-L. Reymond, *J. Chem. Inf. Model.* **52**, 2864 (2012).
- [28] O. A. von Lilienfeld, *International Journal of Quantum Chemistry* **113**, 1676 (2013).
- [29] Y. Okada and Y. Tokumaru, *J. Appl. Phys.* **56**, 314 (1984).
- [30] B. Farid and R. Godby, *Phys. Rev. B* **43**, 14248 (1991).
- [31] R. F. Bader, *Atoms in molecules* (Wiley Online Library, 1990).
- [32] B. Huang and O. A. von Lilienfeld, *J. Chem. Phys.* **145**, 161102 (2016).
- [33] S. Lu, J. Pan, A. Huang, L. Zhuang, and J. Lu, *Proc. Natl. Acad. Sci. USA* **105**, 20611 (2008).
- [34] T. James, D. J. Wales, and J. Hernández-Rojas, *Chem. Phys. Lett.* **415**, 302 (2005).
- [35] O. Loboda and V. Goncharuk, *Chem. Phys. Lett.* **484**, 144 (2010).
- [36] K. Mao, L. Li, W. Zhang, Y. Pei, X. C. Zeng, X. Wu, and J. Yang, *Sci. Rep.* **4**, 5441 (2014).
- [37] K.-R. Müller, M. Finke, N. Murata, K. Schulten, and S. Amari, *Neural Comput.* **8**, 1085 (1996).
- [38] C. Perlich, in *Encyclopedia of Machine Learning* (Springer, 2011) pp. 577–580.
- [39] N. J. Browning, R. Ramakrishnan, O. A. von Lilienfeld, and U. Roethlisberger, *J. Phys. Chem. Lett.* **8**, 1351 (2017).
- [40] A. Pérez, M. E. Tuckerman, H. P. Hjalmarson, and O. A. von Lilienfeld, *J. Am. Chem. Soc.* **132**, 11510 (2010).
- [41] E. Prodan and W. Kohn, *Proc. Natl. Acad. Sci. USA* **102**, 11635 (2005).
- [42] M. G. Medvedev, I. S. Bushmarinov, J. Sun, J. P. Perdew, and K. A. Lyssenko, *Science* **355**, 49 (2017).